Growth and characterization of rare-earth monosulfides for cold cathode applications

Y. Modukuru, J. Thachery, H. Tang, A. Malhotra, M. Cahay,[a] and P. Boolchand
Department of Electrical and Computer Engineering and Computer Science, University of Cincinnati, Cincinnati, Ohio 45221

(Received 27 February 2001; accepted 6 August 2001)

We report the successful growth of bulk cubic lanthanum sulfide (LaS) and neodymium sulfide (NdS). Powder x-ray diffraction scans of the samples show the rocksalt phase with a lattice constant $a_0 = 5.857(2)$ Å and 5.694(2) Å for LaS and NdS, respectively. In Raman scattering, one observes the vibrational density of states (cubic symmetry) and identifies the longitudinal optical and transverse acoustic phonons at 261(284) and 100(92) cm^{-1} with LaS(NdS), respectively. These rare-earth monosulfides offer attractive alternatives to the commonly used cesiated surfaces to reach negative electron affinity at various III–V semiconductor surfaces. © *2001 American Vacuum Society.* [DOI: 10.1116/1.1406158]

I. INTRODUCTION

Over the last 30 yrs, a large number of cold cathode and photocathode structures with semiconductor materials have been proposed.[1,2] Negative electron affinity (NEA) in such structures is achieved by interfacing a wide band gap semiconductor with a low work function (WF) material such that the surface vacuum barrier is brought below the bulk conduction band edge.[3] Cold cathode emitters find applications in a variety of electronic devices, including microwave vacuum transistors and tubes, pressure sensors, thin panel displays, and high temperature and radiation tolerant sensors.

For an electron emitter to be useful in practical applications it should be chemically stable and provide uniform current densities for operational lifetimes over 10^5 h. Alkali metal (Cs) films on emitter surfaces are widely used to lower electronic WF.[3] However, cesiated semiconductor surfaces have several limitations including poor chemical stability of cesium upon releasing bonding electrons, a low melting point (28.5 °C), and high vapor pressure (10^{-3} Torr at 100 °C). Furthermore, accelerated cathode degradation occurs under high current operating conditions due to electron stimulated desorption of the Cs+O activation layer. In general, cesiated surfaces of III–V semiconductors are not stable in an ultrahigh vacuum (UHV). At 300 K, Cs will slowly desorb from the surface in UHV at a rate dependent, in part, on the partial pressure of Cs within the vacuum system. This effect must be compensated by a continuous cesiation during operation of the source.

We recently suggested a more stable approach to reach NEA at semiconductor surfaces based on the use of chalcogenides of the rare-earth elements.[4,5] The possibility was analyzed theoretically based on a local-density approximation to density-functional theory to calculate the WF of the rocksalt phase of LaS and NdS.[6,7] We also proposed and analyzed a new InP/CdS/LaS cold cathode based on this concept[4,5] which can provide emission current densities of several tens of A/cm^2.

Rare-earth monosulfides are unusual in many respects. Not only do they possess high chemical stability (melting temperatures above 2000 °C), but they also display metallic conduction. Material properties of select cubic rare-earth sulfides are summarized in Table I. Of particular interest is the fact that the room temperature WF of these compounds, when extrapolated from high-temperature measurements,[8] is quite small, suggesting that when deposited on *p*-type doped semiconductors these materials can be used to reach NEA. LaS has a lattice constant (5.854 Å) very close to that of InP (5.8688 Å), while NdS has a lattice constant (5.69 Å) very close to that of GaAs (5.6533 Å). Since at room temperature, the WF of LaS (1.14 eV) and NdS (1.36 eV) is, respectively, below the band gap of InP (1.35 eV) and GaAs (1.41 eV),[9] NEA can therefore be realized at InP/LaS and GaAs/NdS interfaces using heavily *p*-type doped semiconductors. Recently, we confirmed these low WF results by means of a first-principles electronic-structure method based on a local-density approximation to density-functional theory.[6,7] The analysis predicts a low-temperature WF of 0.9 and 1.1 eV for LaS and NdS, respectively.

The feasibility to build such cold cathode device structures requires that high purity cubic LaS and NdS in bulk form be readily grown and their work function be established. Such bulk material could then also be used to vapor deposit thin films on suitable semiconductor surfaces and establish the WF in a thin-film configuration. Hereafter, we report on successful growth of cubic bulk LaS and NdS, and have characterized their structure and vibrational density of states by x-ray diffraction (XRD) and Raman scattering. Growth of the cubic phase in its pure form is not obvious. Not only are the melting points of the elements (La, Nd, S) much lower than that of the cubic phase but also the equilibrium phase diagram reveals the presence of several other crystalline phases such as R_2S_3, R_3S_4, and R_2O_2S (with R=La or Nd) that can not only readily form but also are quite stable at elevated temperatures. Here, for the first time that the principal impurity phase R_2O_2S that invariably forms

[a]Electronic mail: mcahay@planck.ececs.uc.edu

TABLE I. Material parameters of some sulfides of rare-earth metals (cubic form): a (lattice constant in Å), WF (work function at room temperature), T_m (melting point in °C), and ρ electrical resistivity (in $\mu\Omega$ cm).[a]

	ErS	YS	NdS	GdS	PrS	CeS	LaS	EuS	SmS
a	5.424	5.466	5.69	5.74	5.747	5.778	5.854	5.968	5.970
WF	⋯	⋯	1.36	⋯	1.26	1.05	1.14	⋯	⋯
T_m	⋯	2060	2200	⋯	2230	2450	2200	⋯	1870
ρ	⋯	⋯	242	⋯	240	170	25	⋯	⋯

[a]See Ref. 8.

upon synthesis of the cubic phase can be completely reduced by carbon addition.

Our experimental approach to grow the cubic LaS and NdS phase is based on reacting equimolar fractions of the rare-earth sesquisulfide with the rare-earth element, by the reaction

$$X_2S_3+X\rightarrow 3XS, \quad (1)$$

where X=La or Nd. The starting materials used in our synthesis, X_2S_3 and X were 99.99% pure (Cerac Inc). In step 1, the starting materials were arc melted taking particular care to handle the starting materials La and La_2S_3. These materials are mixed in stoichiometric amount in a dry N_2 gas ambient in a glove box. The compound is then rapidly transfered to an arc melting chamber flushed with argon. Partial oxidation of the sample can result in the formation of the impurity phase La_2O_2S, which is extremely stable and has a high melting point.

Powder XRD scans of LaS and NdS samples taken with a D-2000 Rigaku powder diffractometer after step 1 reveal the principal reflections of the cubic rocksalt phase (see Fig. 1). A line shape analysis of the reflections yield lattice parameters $a_0=5.857(2)$ and 5.694(2) Å, for LaS and NdS, respectively. These values are in good agreement with earlier reports in the literature.[8,10] The XRD scans [Fig. 1(a)] also reveal traces of an impurity phase which gives rise to minor reflections marked B. The latter reflections can be identified by the oxysulfide phase La_2O_2S (parallel results are obtained with our NdS bulk samples with the presence of the Nd_2O_2S oxysulfide phase).[11] Upon further reaction of the samples with a predetermined amount of intimately mixed carbon (fine powder) in a vacuum oven (10^{-6} Torr) at 1600 °C for 4 h (step 2), the impurity phase could be completely removed. The oxysulfide phase is reduced by carbon to the rocksalt phase according to the chemical reaction

$$X_3S_4+X_2O_2S+2C\rightarrow 5XS+2CO. \quad (2)$$

The precise amount of carbon was determined by trial and error until the presence of the oxysulfide reflections in the XRD scans were completely suppressed,[12] as illustrated in Fig. 1(b). Even though we could not precisely measure the amount of carbon left in the sample, we believe it does not contribute to the second phase observed in the x ray (inset of Fig. 1). The two peaks are due to the $K\alpha_1$ and $K\alpha_2$ lines. The larger lattice constant (leftmost peak in the inset of Fig. 1) comes from material which is S deficient. This could represent the contribution from a remnant of La_3S_4 in the samples, even after the carbon reduction process. Parallel results were obtained upon processing NdS samples.

At the end of step 2, LaS and NdS samples turned *golden yellow* in color. Optical viewing of the materials was performed in our micro-Raman system using an optical micrograph attachment.[13] The samples were not polished and the micrographs were taken from the center of the arc melted boule. Optical viewing of the materials showed gold colored platelets/crystallites (LaS, NdS) with size varying from a few to several tens of microns across. We do not believe the

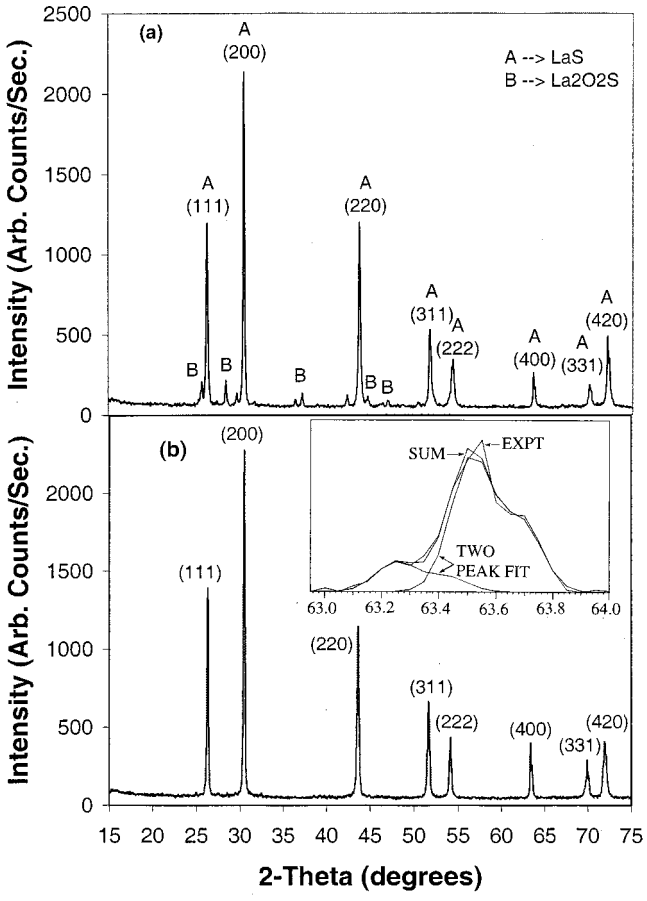

FIG. 1. (a) XRD scan of a LaS sample after the arc melting process. The Bragg reflections due to the cubic LaS phase are identified by Miller indices. The Bragg reflections due to the La_2O_2S impurity phase are identified with the letter B. (b) Same as (a) after the carbon reduction step. The peaks due to the La_2O_2S impurity phase have disappeared. As shown in the inset, some of the Bragg reflection peaks are best approximated by a two-peak fit. The two peaks are due to the $K\alpha_1$ and $K\alpha_2$ lines.

S-poor phase detected in the XRD measurements is at the surface of the gold platelets/crystallites. The LaS and NdS materials are highly conducting and our micro-Raman measurements really probe the surface of the materials. These micro-Raman measurements would be sensitive to a S-deficient phase. This was not observed since the micro-Raman spectra of the gold platelets are consistent with the cubic phase of LaS and NdS, as discussed below.

Close examination of the Bragg reflections required a two-peak deconvolution [see inset of Fig. 1(b)] suggesting the presence of a majority LaS phase [$a_0 = 5.857(2)$ Å] and a minority LaS phase [$a_0 = 5.875(2)$ Å] in our samples. A similar two-peak deconvolution was also found to work well for the NdS samples. The lattice constants (a_0) given here correspond to those of the majority phase. The two sets of reflections may come from a S-rich and a S-poor phase present in the samples with the S-poor phase possessing a somewhat larger lattice constant. These results clearly suggest that the cubic phase can be stabilized over a range of La:S stoichiometry, as is known from the phase diagram. In these XRD scans, the typical full width at half maximum is found to be 0.14° for LaS and 0.19° for NdS. These are close to the instrumental resolution (0.12°) of our Rigaku powder diffractometer. These results suggest that the samples obtained in the present synthesis are rather well crystallized and it is likely that upon melting the samples at elevated temperatures (above 220 °C) one may obtain rather homogeneous samples. This is a subject of current investigations.

The formation of the bulk material in its highest purity form is of interest to us since the materials will eventually be used to form targets for rf magnetron sputtering of thin films on various III–V substrates as discussed above. To ensure reproducibility of the deposition, a fixed starting stoichiometry is desirable. Given the stability of LaS and NdS, the bulk material would appear to be a useful cathode material. Our experience with a stoichiometric CdS target shows that stoichiometric CdS thin film can be grown by rf sputtering.[12] It is therefore quite likely that the same procedure would work for deposition of LaS and NdS thin films. In particular, the experimental conditions (argon pressure, rf power, and substrate temperature) established for CdS thin films[12] could serve as a guide in LaS and NdS thin-film deposition by rf sputtering. Detailed results will be published elsewhere.

Cubic LaS and NdS in the rocksalt structure should display three zone center optical modes which should be Raman silent because of inversion symmetry. The modes observed in Raman scattering (Fig. 2) are either due to noncubic impurity phases or to defect induced first order scattering, which activates all vibrational modes in the Brillouin zone of the cubic phase to yield the full vibrational density of states (VDOS). Raman scattering was performed with a model T64000 triple monochromator system from Instruments SA Inc., equipped with a microscope and a charge-coupled device detector.[13] In these micro-Raman measurements the exciting laser beam, focused to a 1 μm spot size, was used to examine large ($50\,\mu\text{m} \times 50\,\mu\text{m}$) LaS and NdS platelets exclusively. The results shown in Fig. 2 were obtained with 4 mW of 514.5 nm radiation used to excite the scattering.

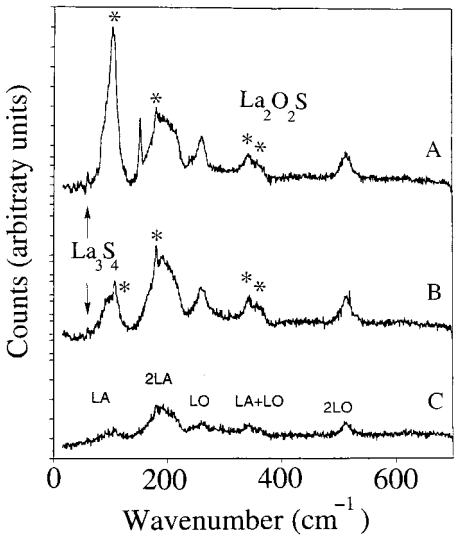

FIG. 2. Raman spectra of an in-house grown LaS bulk sample processed in a Ta crucible using the two-step procedure described in the text. Scans A, B, and C correspond to an amount C/LaS weight ratio in the carbon reduction process equal to 0.3%, 0.7%, and 2.5%, respectively. In the bottom sample, the oxysulfide phase has disappeared in the XRD spectrum of the sample. The acoustic and optical phonon modes and some of their overtones are clearly identified. Some of the impurity phases responsible for some of the sharp modes observed in the top two spectra are also identified: the star corresponds to the La_2O_2S phase and the arrows indicate the La_3S_4 phase. The micro-Raman measurements were performed at 300 K using the 514.5 nm exciting line of an argon laser with the same power levels (2.5 mW) in all three scans.

The Raman scattering (RS) results on LaS and NdS samples complement the XRD results. In RS, we observe changes in the VDOS due to a change in structure. In Fig. 2 scans A, B, and C correspond to samples reduced in step 2 with a C/LaS weight ratio of 0.3%, 0.7%, and 2.5%, respectively. The sample reduced with 2.5% C (scan C) displayed very weak scattering. This particular sample showed the complete absence of the La_2O_2S phase in the XRD measurements. The RS scans A and B show the presence of sharp peaks, which can be identified with the impurity phases (La_2O_2S, La_3S_4) present in these samples.[14] We are not sure of the origin of the 180 cm^{-1} mode, which has been observed on occasions. Since these impurity phases are noncubic, the Raman scattering from these phases is rather strong. In scan C, however, the sharp modes are absent, the scattering is extremely weak, and the vibrational modes are rather broad (vibrational bands). These features of Raman scattering are characteristic of the VDOS of the cubic phase. These results are consistent with an improvement in sample quality due to carbon reduction. The observed modes in scan C can be identified with specific phonons in the VDOS of the rocksalt phase.

In LaS and NdS, the cation–anion mass ratio is close to 5:1. This permits the optic branch to be clearly separated from the acoustic one. In LaS samples, we identify the 261 cm^{-1} vibrational band with the longitudinal optical (LO) phonon, the 100 cm^{-1} band with the acoustic phonon (A),

TABLE II. Observed acoustic and optical phonon energies (in cm^{-1}) in cubic phase of rare-earth metals.

Host	Acoustic	Optical
LaS	100	261
NdS	92	284

and the remaining vibrational bands as two-phonon modes (acoustic+optical) and 2 LO mode. These results are in good agreement with an earlier article,[15] where the LO mode and *A* mode were identified at 268 and 96 cm^{-1}, respectively. Similar vibrational modes are observed in NdS: acoustic 2*A* and LO phonons at 92, 195, and 284 cm^{-1}, respectively. Since the atomic mass of La (138.9 amu) is less than that of Nd (144.24), the 6% larger value of the observed LO phonon frequency in NdS is a rather curious result. It is possible that it results from a larger force constant due to the smaller lattice constant of the NdS unit cell (Table II). On the other hand, the lower frequency of the *A* phonon in NdS compared to that in LaS could possibly derive from the unusual phonon dispersion $\omega(k)$, leading to a softening of this mode as suggested by Steiner and co-workers.[16]

To conclude, we have identified a process to successfully grow pure LaS and NdS in the rocksalt phase. For the first time, we were able to remove the oxysulfide impurity phase (X_2O_2S, X=La or Nd) present in the samples using a high-temperature carbon reduction process. The successful removal of the oxysulfide phase was supported by the absence of sharp phonon modes in Raman scattering experiments. This successful growth of extremely pure rare-earth monosulfides is the crucial step if thin films of these materials are to be used as more stable alternatives to Cs to reach NEA at the surface of semiconductor compounds. The procedure described here could be used to grow other rare-earth monosulfides but LaS and NdS have the advantage of a close lattice match to the most widely used III–V semiconductors, as illustrated in Table I.

ACKNOWLEDGMENTS

This work is supported by the National Science Foundation under Award No. ECS-9906053. This work is also partially supported by the Air Force Research Laboratory, Sensors Directorate, at Wright-Patterson Air Force Base under Contract No. F33615-98-C-1204.

[1]S. Iannazzo, Solid-State Electron. **36**, 301 (1993).
[2]I. Brodie and C. A. Spindt, *Advance in Electronics and Electron Physics* (Academic, New York, 1992), Vol. 83, p. 2.
[3]P. R. Bell, *Negative Electron Affinity Devices* (Clarendon, Oxford, 1973).
[4]P. D. Mumford and M. Cahay, J. Appl. Phys. **79**, 2176 (1996).
[5]P. D. Mumford and M. Cahay, J. Appl. Phys. **81**, 3707 (1997).
[6]O. Eriksson, J. Willis, P. D. Mumford, M. Cahay, and W. Friz, Phys. Rev. B **57**, 4067 (1998).
[7]O. Eriksson and M. Cahay (unpublished).
[8]G. V. Samsonov, *High Temperature Compounds of Rare-Earth Metals with Nonmetals* (Consultants Bureau, New York, 1965).
[9]The room temperature work function for LaS and NdS was calculated by extrapolating measured work function values at high temperature as reported by S. Fomenko, in *Handbook of Thermionic Properties* (Plenum, New York, 1966). Within the range of temperature investigated by Fomenko, the work function increases with temperature at a rate of a few meV/K.
[10]A. V. Golubkov, T. B. Zhukova, and V. M. Sergeeva, Izv. Akad. Nauk SSSR, Neorg. Mater. **2**, 77 (1966).
[11]Joint Committee of Powder Diffraction Standards: card 27-321 for Nd_2O_2S and cards 27-263 and 22-370 for La_2O_2S.
[12]H. Tang, Masters thesis, University of Cincinnati, Cincinatti, Ohio, 1999.
[13]The LaS and NdS bulk samples were examined in a micro-Raman equipped with an optical microscope attachment with a video monitor. Examples of sample micrographs can be viewed at the following website address: http:www.ececs.uc.edu/~mcahay/cathodes2.html.
[14]A. Malhotra, Masters thesis, University of Cincinnati, Cincinatti, Ohio, 1999.
[15]I. Frankowski and P. Watcher, Solid State Commun. **40**, 885 (1981).
[16]M. M. Steiner, H. Eschring, and R. Monnier, Phys. Rev. B **45**, 7183 (1992).